Eur. Phys. J. B **5**, 351–359 (1998)

THE EUROPEAN PHYSICAL JOURNAL B

Elementary excitations for the Anderson model at finite temperatures*

A. Tomiyama[1], S. Suga[1,a], and A. Okiji[2]

[1] Department of Applied Physics, Osaka University, Suita, Osaka 565, Japan
[2] Wakayama National College of Technology, Gobo, Wakayama 644, Japan

Received: 21 January 1998 / Accepted: 17 March 1998

Abstract. The elementary excitation spectrums for the Anderson model at finite temperatures are calculated by using the Bethe-ansatz solution. The formulation is based on the method of Yang and Yang, which was developed for the one-dimensional boson systems with the δ-function type interaction. We obtain the temperature dependence of the spin and the charge excitation spectrums. When the impurity level lies deeply from the Fermi level and the Coulomb interaction is suitably large, the resonant peak structure develops in the low energy region of the spin excitation spectrum and the hump structure grows around the impurity level of the charge excitation spectrum with decreasing temperature.

PACS. 75.20.Hr Local moment in compounds and alloys; Kondo effect, valence fluctuations, heavy fermions – 72.15.Qm Scattering mechanisms and Kondo effect – 71.27.+a Strongly correlated electron systems; heavy fermions

1 Introduction

The single-impurity Anderson model has been studied intensively for years as one of the most important Hamiltonian of the condensed-matter physics. Indeed, this model has been applied to investigate, for example, the Kondo problem [1,2], the physics of actinide and rare-earth compounds [3] and the dynamical process of an adsorbed atom on metal surfaces [4]. Considerable progress in understanding the physical properties of the model has been achieved by various theoretical methods such as the perturbative approach [5], the renormalization-group approach [6] and the Bethe ansatz solution [7,8].

The physical property of the Anderson model depends mainly on the strength of the Coulomb interaction between the electrons of the localized orbital and the energy level of the impurity. When the Coulomb interaction is suitably large and the impurity level lies deeply below the Fermi level, we observe the Kondo effect in this model at low temperatures. If the impurity level approaches to the Fermi level, the Kondo effect disappears and the ground state with intermediate valence comes out. In fact, physical quantities such as the spin susceptibility and the specific heat in both cases show characteristic temperature dependences [9,10].

The elementary excitation spectrums at finite temperatures provide us with an important information about the correlation effects of the systems at finite temperatures. Some calculations of the single particle spectral-densities at finite temperatures have been performed for the Anderson model based on the quantum Monte-Carlo method [11] and the numerical renormalization-group method [12, 13], and the temperature dependence of peak structures has been discussed. In this paper, we calculate the elementary excitation spectrums of the Anderson model at finite temperatures by using the Bethe ansatz solution. Following the method of Yang and Yang [14], we introduce a dressed particle to formulate the elementary excitation at finite temperatures, which is a local analogue of the collective mode in the periodic system such as the des Cloizeaux and Pearson mode for the one-dimensional Heisenberg antiferromagnet [15]. Note that the elementary excitation spectrums of the quantum impurity problems obtained by this method show behaviors characteristic of the local correlation effect of the system at finite temperatures [16]. In the calculation of the excitation spectrums for the Anderson model at zero temperature, the spin and the charge degrees of freedom have been treated independently [17], although the Anderson model is known to exhibit the local Fermi-liquid properties concerning the low-energy excitation. This does not contradict each other. It has been shown that the local Fermi-liquid is always stabilized due to the locality of the correlation, though the spin-charge separation occurs even in the Kondo system [18]. We consider that this is true also at low temperatures.

The set-up of the present paper is as follows. In Section 2, we summarize briefly the thermodynamic Bethe ansatz method for the Anderson model. In Section 3,

* Dedicated to J. Zittartz on the occasion of his 60th birthday

[a] e-mail: suga@dyn.ap.eng.osaka-u.ac.jp

we formulate the elementary excitations for the spin and the charge degrees of freedom at finite temperatures. Numerical results for the spectral density are presented in Section 4. Section 5 is devoted to the summary of this paper.

2 Bethe ansatz equations at finite temperatures

We first recapitulate the exact solution of the Anderson model at finite temperatures. The Anderson model describes free conduction electrons coupled with correlated d-electrons at the impurity through the resonant hybridization. The Hamiltonian is described as

$$H = \sum_{k\sigma} \epsilon_k c^\dagger_{k\sigma} c_{k\sigma} + \sum_{k\sigma} V_k (c^\dagger_{k\sigma} d_\sigma + d^\dagger_\sigma c_{k\sigma}) + \epsilon_d \sum_\sigma d^\dagger_\sigma d_\sigma + U d^\dagger_\uparrow d_\uparrow d^\dagger_\downarrow d_\downarrow. \quad (1)$$

Under the condition that only the s-wave component of the conduction electron is mixed with the localized electron, the model can be reduced to one dimension. We linearlize the dispersion as $\epsilon_k = vk$ with $v = 1$ near the Fermi level and convert the kinetic energy into $-i\partial/\partial x$ in the coordinate representation. Due to these simplification, the Hamiltonian can be diagonalized exactly by the Bethe ansatz method [7]. The Bethe ansatz equations are given as

$$e^{ik_j L} = \left[\prod_{\alpha=1}^{M} \frac{B(k_j) - \Lambda_\alpha + iU\Delta}{B(k_j) - \Lambda_\alpha - iU\Delta} \right] \cdot \frac{k_j - \epsilon_d + i\Delta}{k_j - \epsilon_d - i\Delta}, \quad (2)$$

$$\prod_{j=1}^{N} \frac{\Lambda_\alpha - B(k_j) + iU\Delta}{\Lambda_\alpha - B(k_j) - iU\Delta} = -\prod_{\beta=1}^{M} \frac{\Lambda_\alpha - \Lambda_\beta + i2U\Delta}{\Lambda_\alpha - \Lambda_\beta - i2U\Delta}, \quad (3)$$

where $B(k_j) = (k_j - U/2 - \epsilon_d)^2$, k_j and Λ_α are the rapidities concerning the charge and the spin degrees of freedom, and the resonance width is given as $\Delta = V^2/2$. The length of the system and the number of electrons (down spin) are denoted as L and $N(M)$, respectively. The ground state of the Anderson model has been proved to be constructed by the bound-state solution of two electrons with the antiparallel spins as [8]

$$k^\pm_\alpha = -\sqrt{\Lambda_\alpha \pm iU\Delta} + U + 2\epsilon_d, \quad (4)$$

where Λ_α is a real spin rapidity. The magnetic excitation is expressed by the real charge rapidity.

At finite temperatures, solutions are grouped into complex spin rapidities, complex charge rapidities and real charge rapidities [19]. The complex spin rapidities are given by two sets of series as

$$\lambda^{n,j}_\alpha = \lambda^n_\alpha + i\,(n+1-2j)\,U\Delta, \quad (n = 1, 2, \dots;\ j = 1, 2, \dots, n), \quad (\alpha = 1, 2, \dots, M'_n) \quad (5)$$

$$\Lambda^{n,j}_\alpha = \Lambda^n_\alpha + i\,(n+1-2j)\,U\Delta, \quad (n = 1, 2, \dots;\ j = 1, 2, \dots, n), \quad (\alpha = 1, 2, \dots, M_n) \quad (6)$$

where $M'_n(M_n)$ is the number of $\lambda^n_\alpha(\Lambda^n_\alpha)$. The complex charge rapidities are related to one of two sets of complex spin rapidities as

$$B(k^{n,j}_\alpha) = \lambda^{n,j}_\alpha \pm iU\Delta. \quad (7)$$

The real parts of these rapidities and the real charge rapidities k_j ($j = 1, 2, \dots, N - 2M'; M' = \sum_{n=1}^{\infty} nM'_n$) satisfy the following equations:

$$k_j L = 2\pi I_j + \sum_{n=1}^{\infty} \left[\sum_{\alpha=1}^{M_n} \theta\left(\frac{B(k_j) - \Lambda^n_\alpha}{nU\Delta} \right) + \sum_{\alpha=1}^{M'_n} \theta\left(\frac{B(k_j) - \lambda^n_\alpha}{nU\Delta} \right) \right] - \phi(k_j), \quad (8)$$

$$\left[2\Re\sqrt{\lambda^n_\alpha + inU\Delta} - 2n(U/2 + \epsilon_d) \right] L = 2\pi K^n_\alpha - \sum_{j=1}^{N-2M'} \theta\left(\frac{\lambda^n_\alpha - B(k_j)}{nU\Delta} \right) - \sum_{m=1}^{\infty} \sum_{\beta=1}^{M'_m} \Theta_{nm}\left(\frac{\lambda^n_\alpha - \lambda^m_\beta}{U\Delta} \right) + p_n(\lambda^n_\alpha), \quad (9)$$

$$-\sum_{j=1}^{N-2M'} \theta\left(\frac{\Lambda^n_\alpha - B(k_j)}{nU\Delta} \right) = 2\pi J^n_\alpha - \sum_{m=1}^{\infty} \sum_{\beta=1}^{M_m} \Theta_{nm}\left(\frac{\Lambda^n_\alpha - \Lambda^m_\beta}{U\Delta} \right), \quad (10)$$

where

$$\theta(x) = -2\tan^{-1} x, \quad (11)$$

$$\Theta_{nm}(x) = \begin{cases} \theta\left(\frac{x}{n+m}\right) + 2\theta\left(\frac{x}{n+m-2}\right) + \cdots \\ +2\theta\left(\frac{x}{|n-m|+2}\right) + \theta\left(\frac{x}{|n-m|}\right) & (n \neq m) \\ \theta\left(\frac{x}{2n}\right) + 2\theta\left(\frac{x}{2n-2}\right) + \cdots + 2\theta\left(\frac{x}{2}\right) & (n = m), \end{cases} \quad (12)$$

$$\phi(x) = -2\tan^{-1}\left(\frac{\Delta}{x - \epsilon_d} \right), \quad (13)$$

$$p_n(\lambda^n_\alpha) = \sum_{j=1}^{n} [\phi(-\sqrt{\lambda^{n,j}_\alpha + iU\Delta} + U/2 + \epsilon_d) + \phi(-\sqrt{\lambda^{n,j}_\alpha - iU\Delta} + U/2 + \epsilon_d)]. \quad (14)$$

Quantum numbers I_j, K_α^n and J_α^n specify k_j, λ_α^n and Λ_α^n, respectively. The total energy is given by

$$E = \sum_{j=1}^{N-2M'} k_j + \sum_{n=1}^{\infty}\sum_{\alpha=1}^{M'_n}[-2\Re\sqrt{\lambda_\alpha^n + inU\Delta} + 2n(U/2+\epsilon_d)]. \quad (15)$$

In the thermodynamic limit, the distributions of the rapidities k_j, λ_α^n and Λ_α^n are described by the functions $\rho(k)$, $\sigma'_n(\Lambda)$ and $\sigma_n(\Lambda)$, respectively, and those of the holes are given by $\rho^h(k)$, $\sigma'^h_n(\Lambda)$ and $\sigma^h_n(\Lambda)$. Equations (8–10) are reduced to the set of integral equations for the distribution functions as

$$\rho(k) + \rho^h(k) = \frac{1}{2\pi} + \frac{1}{L}\varphi(k) + B'(k)\sum_{n=1}^{\infty}\int_{-\infty}^{\infty} d\Lambda F_n(B(k)-\Lambda)[\sigma_n(\Lambda) + \sigma'_n(\Lambda)], \quad (16)$$

$$\sigma'^h_n(\Lambda) = \frac{1}{2\pi}\left(\frac{d}{d\Lambda}2\Re\sqrt{\Lambda + inU\Delta}\right) - \frac{1}{2\pi L}\frac{d}{d\Lambda}p_n(\Lambda) - \int_{-\infty}^{\infty} dk F_n(\Lambda - B(k))\rho(k) - \sum_{m=1}^{\infty} A_{nm}(\Lambda) * \sigma'_m(\Lambda), \quad (17)$$

$$\sigma^h_n(\Lambda) = \int_{-\infty}^{\infty} dk F_n(\Lambda - B(k))\rho(k) - \sum_{m=1}^{\infty} A_{nm}(\Lambda) * \sigma_m(\Lambda), \quad (18)$$

where asterisk denotes convolution, and

$$B'(k) = \frac{d}{dk}B(k), \quad (19)$$

$$F_n(x) = \frac{1}{\pi}\frac{nU\Delta}{x^2 + (nU\Delta)^2}, \quad (20)$$

$$A_{nm}(x) = \delta_{nm}\delta(x) + \frac{1}{2\pi}\frac{d}{dx}\Theta_{nm}(\frac{x}{U\Delta}), \quad (21)$$

$$\varphi(x) = \frac{1}{\pi}\frac{\Delta}{(x-\epsilon_d)^2 + \Delta^2}\,. \quad (22)$$

At temperature T ($k_B = 1$), the distribution functions at thermal equilibrium have to be determined by minimizing the thermodynamic potential $\Omega = E - TS$, where S is the entropy. From the condition $\delta\Omega = 0$, the following equations are derived [9,10,19,20]:

$$\frac{\kappa(k)}{T} = \frac{k}{T} - \sum_{n=1}^{\infty}\int_{-\infty}^{\infty} d\Lambda F_n(B(k)-\Lambda) \times \left[\ln\left(1+e^{-\varepsilon_n(\Lambda)/T}\right) - \ln\left(1+e^{-\varepsilon'_n(\Lambda)/T}\right)\right], \quad (23)$$

$$\ln\left(1+e^{\varepsilon'_n(\Lambda)/T}\right) = \frac{-2\Re\sqrt{\Lambda + inU\Delta} + 2n(U/2+\epsilon_d)}{T} - \int_{-\infty}^{\infty} dk B'(k)F_n(\Lambda - B(k))\ln\left(1+e^{-\kappa(k)/T}\right) + \sum_{m=1}^{\infty} A_{nm}(\Lambda) * \ln\left(1+e^{-\varepsilon'_m(\Lambda)/T}\right), \quad (24)$$

$$\ln\left(1+e^{\varepsilon_n(\Lambda)/T}\right) = -\int_{-\infty}^{\infty} dk B'(k)F_n(\Lambda - B(k)) \times \ln\left(1+e^{-\kappa(k)/T}\right) + \sum_{m=1}^{\infty} A_{nm}(\Lambda) * \ln\left(1+e^{-\varepsilon_m(\Lambda)/T}\right), \quad (25)$$

where $\kappa(k) = T\ln(\rho^h(k)/\rho(k))$, $\varepsilon'_n(\Lambda) = T\ln(\sigma'^h_n(\Lambda)/\sigma'_n(\Lambda))$ and $\varepsilon_n(\Lambda) = T\ln(\sigma^h_n(\Lambda)/\sigma_n(\Lambda))$ are pseudo-energies. The equations (23–25) are the Bethe ansatz solutions of the Anderson model at finite temperatures.

3 Elementary excitations

To calculate the elementary excitations for the spin and the charge degrees of freedom at finite temperatures, let us recall here that the ground state is expressed by the bound-state solution of two electrons which is determined by the real spin rapidity, and that the magnetic excitation is determined by the real charge rapidity [8]. Furthermore, the impurity contribution to the free-energy functional at thermal equilibrium is expressed by the real spin rapidity which describes the bound state of two electrons, and the real charge rapidity [9,10,19,20]. Therefore, low-energy properties of the model are mainly controlled by the real spin and charge rapidities mentioned above. Based on these observations, it is considered that the spin excitation at finite temperatures is obtained by adding one real charge rapidity at thermal equilibrium, and that the charge excitation at finite temperatures is obtained by removing a pair of bound-state solutions at thermal equilibrium, respectively, with the total electron number being fixed. These are referred to as a dressed-particle excitation and a dressed-hole excitation, respectively. Following the method of Yang and Yang [14], we derive the formulation for the shift of the energy from that of thermal equilibrium, which is defined as the excitation energy at finite temperatures.

3.1 Spin excitation

First, we calculate the spin excitation. As mentioned above, we insert a hole into the real charge rapidity at k_h or the corresponding quantum number I_h, and add a particle to the real charge rapidity at k_p or I_p, other quantum numbers remaining unchanged. Due to this procedure, the distribution of rapidities is rearranged through the phase

shift in (8–10). This is the back-flow effect. After the excitation, the basic equations (8–10) are expressed in terms of $\{k'_j\}, \{\lambda^{n\prime}_\alpha\}$ and $\{\Lambda^{n\prime}_\alpha\}$, where $\{k'_j\}, \{\lambda^{n\prime}_\alpha\}$ and $\{\Lambda^{n\prime}_\alpha\}$ are the new sets of rapidities. We write the shifts of rapidities as

$$\frac{1}{L}\Delta k_j = k'_j - k_j, \tag{26}$$

$$\frac{1}{L}\Delta\lambda^n_\alpha = \lambda^{n\prime}_\alpha - \lambda^n_\alpha, \tag{27}$$

$$\frac{1}{L}\Delta\Lambda^n_\alpha = \Lambda^{n\prime}_\alpha - \Lambda^n_\alpha. \tag{28}$$

Since the shifts of rapidities are sufficiently small, we take into account only the lowest order of them. Expanding the basic equations (8–10) in terms of the shifts of rapidities, we obtain the following equations:

$$\begin{aligned}&\left[\frac{1}{2\pi}+\frac{1}{L}\phi(k_j)\right]\Delta k_j \\ &= -\frac{1}{L}\sum_{n=1}^{\infty}\left[\sum_{\alpha=1}^{M_n}F_n(B(k_j)-\Lambda^n_\alpha)\cdot(B'(k_j)\Delta k_j-\Delta\Lambda^n_\alpha)\right. \\ &\quad\left.+\sum_{\alpha=1}^{M'_n}F_n(B(k_j)-\lambda^n_\alpha)\cdot(B'(k_j)\Delta k_j-\Delta\lambda^n_\alpha)\right],\end{aligned} \tag{29}$$

$$\begin{aligned}&\left\{\frac{1}{\pi}\left(\frac{d}{d\lambda^n_\alpha}\Re\sqrt{\lambda^n_\alpha+inU\Delta}\right)-\frac{1}{L}\left[\frac{d}{d\lambda^n_\alpha}p_n(\lambda^n_\alpha)\right]\right\}\Delta\lambda^n_\alpha \\ &= \frac{1}{L}\sum_{j=1}^{N-2M'}F_n(\lambda^n_\alpha-B(k_j))\cdot(\Delta\lambda^n_\alpha-B'(k_j)\Delta k_j) \\ &\quad+\frac{1}{L}\sum_{m=1}^{\infty}\sum_{\beta=1}^{M'_m}B_{nm}(\lambda^n_\alpha-\lambda^m_\beta)\cdot(\Delta\lambda^n_\alpha-\Delta\lambda^m_\beta) \\ &\quad-\frac{1}{2\pi}\left[\theta\left(\frac{\lambda^n_\alpha-B(k_p)}{nU\Delta}\right)-\theta\left(\frac{\lambda^n_\alpha-B(k_h)}{nU\Delta}\right)\right],\end{aligned} \tag{30}$$

$$\begin{aligned}&\frac{1}{L}\sum_{j=1}^{N-2M'}F_n(\Lambda^n_\alpha-B(k_j))\cdot(\Delta\Lambda^n_\alpha-B'(k_j)\Delta k_j) \\ &= \frac{1}{L}\sum_{m=1}^{\infty}\sum_{\beta=1}^{M_m}B_{nm}(\Lambda^n_\alpha-\Lambda^m_\beta)\cdot(\Delta\Lambda^n_\alpha-\Delta\Lambda^m_\beta) \\ &\quad+\frac{1}{2\pi}\left[\theta\left(\frac{\Lambda^n_\alpha-B(k_p)}{nU\Delta}\right)-\theta\left(\frac{\Lambda^n_\alpha-B(k_h)}{nU\Delta}\right)\right],\end{aligned} \tag{31}$$

where $B_{nm}(x) = A_{nm}(x) - \delta_{nm}\delta(x)$. In the thermodynamic limit, these equations turn into integral equations for $\Delta k(k)$, $\Delta\lambda_n(\Lambda)$ and $\Delta\Lambda_n(\Lambda)$ as

$$\begin{aligned}&[\rho(k)+\rho^h(k)]\Delta k(k) = \sum_{n=1}^{\infty}\int_{-\infty}^{\infty}d\Lambda F_n(B(k)-\Lambda) \\ &\times[\sigma_n(\Lambda)\Delta\Lambda_n(\Lambda)+\sigma'_n(\Lambda)\Delta\lambda_n(\Lambda)],\end{aligned} \tag{32}$$

$$\begin{aligned}&\sigma'^h_n(\Lambda)\Delta\lambda_n(\Lambda) = \\ &-\int_{-\infty}^{\infty}dkB'(k)F_n(\Lambda-B(k))\rho(k)\Delta k(k) \\ &-\sum_{m=1}^{\infty}A_{nm}(\Lambda)*[\sigma'_m(\Lambda)\Delta\lambda_m(\Lambda)] \\ &-\frac{1}{2\pi}\left[\theta\left(\frac{\Lambda-B(k_p)}{nU\Delta}\right)-\theta\left(\frac{\Lambda-B(k_h)}{nU\Delta}\right)\right],\end{aligned} \tag{33}$$

$$\begin{aligned}&\sigma^h_n(\Lambda)\Delta\Lambda_n(\Lambda) = \\ &\int_{-\infty}^{\infty}dkB'(k)F_n(\Lambda-B(k))\rho(k)\Delta k(k) \\ &-\sum_{m=1}^{\infty}A_{nm}(\Lambda)*[\sigma_m(\Lambda)\Delta\Lambda_m(\Lambda)] \\ &+\frac{1}{2\pi}\left[\theta\left(\frac{\Lambda-B(k_p)}{nU\Delta}\right)-\theta\left(\frac{\Lambda-B(k_h)}{nU\Delta}\right)\right].\end{aligned} \tag{34}$$

In this way, the shifts of rapidities due to the back-flow effect are determined completely.

We now calculate the energy increment associated with the elementary excitation. The excitation energy is given by the sum of the bare energy shift and the energy shift due to the back-flow effect:

$$\begin{aligned}&\epsilon_s(k_p,k_h) = k_p - k_h + \int_{-\infty}^{\infty}dk\rho(k)\Delta k(k) \\ &+\sum_{n=1}^{\infty}\int_{-\infty}^{\infty}d\Lambda\sigma'_n(\Lambda)\Delta\lambda_n(\Lambda) \\ &\times\left\{\frac{d}{d\Lambda}\left[-2\Re\sqrt{\Lambda+inU\Delta}\right]\right\}.\end{aligned} \tag{35}$$

Differentiating the equations (23–25) with respect to the rapidities, and substituting them into the expression (35),

we obtain

$$\begin{aligned}
&\epsilon_s(k_p,k_h)= \\
&\int_{-\infty}^{\infty}dk\frac{\frac{d}{dk}\kappa\left(k\right)}{1+e^{\kappa(k)/T}}\Big[(1+e^{\kappa(k)/T})\rho\left(k\right)\Delta k\left(k\right) \\
&-\sum_{n=1}^{\infty}\int_{-\infty}^{\infty}d\Lambda F_n(B(k)-\Lambda)\{\sigma_n\left(\Lambda\right)\Delta\Lambda_n\left(\Lambda\right) \\
&+\sigma_n'\left(\Lambda\right)\Delta\lambda_n\left(\Lambda\right)\}\Big] \\
&+\sum_{n=1}^{\infty}\int_{-\infty}^{\infty}d\Lambda\frac{\frac{d}{d\Lambda}\varepsilon_n'\left(\Lambda\right)}{1+e^{\varepsilon_n'(\Lambda)/T}}\Big[e^{\varepsilon_n'(\Lambda)/T}\sigma_n'\left(\Lambda\right)\Delta\lambda_n\left(\Lambda\right) \\
&+\int_{-\infty}^{\infty}dkB'(k)F_n(\Lambda-B(k))\rho\left(k\right)\Delta k\left(k\right) \\
&+\sum_{m=1}^{\infty}A_{nm}(\Lambda)*\{\sigma_m'\left(\Lambda\right)\Delta\lambda_m\left(\Lambda\right)\}\Big] \\
&+\sum_{n=1}^{\infty}\int_{-\infty}^{\infty}d\Lambda\frac{\frac{d}{d\Lambda}\varepsilon_n\left(\Lambda\right)}{1+e^{\varepsilon_n(\Lambda)/T}}\Big[e^{\varepsilon_n(\Lambda)/T}\sigma_n\left(\Lambda\right)\Delta\Lambda_n\left(\Lambda\right) \\
&-\int_{-\infty}^{\infty}dkB'(k)F_n(\Lambda-B(k))\rho\left(k\right)\Delta k\left(k\right) \\
&+\sum_{m=1}^{\infty}A_{nm}(\Lambda)*\{\sigma_m\left(\Lambda\right)\Delta\Lambda_m\left(\Lambda\right)\}\Big]. \qquad (36)
\end{aligned}$$

Using the equations (32–34), we find finally the simple formula for the excitation energy renormalized by the back-flow effect, as

$$\epsilon_s(k_p,k_h)=\kappa(k_p)-\kappa(k_h). \qquad (37)$$

It is noted that the spin excitation energy can be described by using only the pseudo-energy for the real charge rapidity at thermal equilibrium. In the limit of $T\to 0$, the expression (37) coincides with the spin excitation energy from the ground state. At finite temperatures, the elementary excitation by other kinds of string solutions can also be formulated. In the limit of $T\to 0$, however, these excitation energies vanish and there remains only the excitation energy for the real charge rapidity.

3.2 Charge excitation

Next we calculate the charge excitation. As mentioned before, the charge excitation is given by treating a bound-state solution which is described by the real spin rapidity. Thus, we insert a hole into the real spin rapidity at λ_h or K_h^1, and add a particle to the real spin rapidity at λ_p or K_p^1. Expanding equations (8–10) in terms of the shifts of rapidities, we obtain the following set of equations to determine $\Delta k\left(k\right)$, $\Delta\lambda_n\left(\Lambda\right)$ and $\Delta\Lambda_n\left(\Lambda\right)$ in the thermodynamic limit:

$$\begin{aligned}
&[\rho\left(k\right)+\rho^h\left(k\right)]\Delta k\left(k\right)= \\
&\sum_{n=1}^{\infty}\int_{-\infty}^{\infty}d\Lambda F_n(B(k)-\Lambda)[\sigma_n\left(\Lambda\right)\Delta\Lambda_n\left(\Lambda\right) \\
&+\sigma_n'\left(\Lambda\right)\Delta\lambda_n\left(\Lambda\right)] \\
&+\frac{1}{2\pi}\left[\theta\left(\frac{B(k)-\lambda_p}{U\Delta}\right)-\theta\left(\frac{B(k)-\lambda_h}{U\Delta}\right)\right], \qquad (38)
\end{aligned}$$

$$\begin{aligned}
&\sigma_n'^h\left(\Lambda\right)\Delta\lambda_n\left(\Lambda\right)= \\
&-\int_{-\infty}^{\infty}dkB'(k)F_n(\Lambda-B(k))\rho\left(k\right)\Delta k\left(k\right) \\
&-\sum_{m=1}^{\infty}A_{nm}(\Lambda)*[\sigma_m'\left(\Lambda\right)\Delta\lambda_m\left(\Lambda\right)] \\
&-\frac{1}{2\pi}\left[\Theta_{n1}(\Lambda-\lambda_p)-\Theta_{n1}(\Lambda-\lambda_h)\right], \qquad (39)
\end{aligned}$$

$$\begin{aligned}
&\sigma_n^h\left(\Lambda\right)\Delta\Lambda_n\left(\Lambda\right)= \\
&\int_{-\infty}^{\infty}dkB'(k)F_n(\Lambda-B(k))\rho\left(k\right)\Delta k\left(k\right) \\
&-\sum_{m=1}^{\infty}A_{nm}(\Lambda)*[\sigma_m\left(\Lambda\right)\Delta\Lambda_m\left(\Lambda\right)]. \qquad (40)
\end{aligned}$$

The excitation energy is given by the sum of the bare energy shift and the energy shift caused by the back-flow effect as

$$\begin{aligned}
&\epsilon_c(\lambda_p,\lambda_h)=-2\sqrt{\lambda_p+iU\Delta}+2\sqrt{\lambda_h+iU\Delta} \\
&+\int_{-\infty}^{\infty}dk\rho\left(k\right)\Delta k\left(k\right)+\sum_{n=1}^{\infty}\int_{-\infty}^{\infty}d\Lambda\sigma_n'\left(\Lambda\right)\Delta\lambda_n\left(\Lambda\right) \\
&\times\left\{\frac{d}{d\Lambda}\left[-2\Re\sqrt{\Lambda+inU\Delta}\right]\right\}. \qquad (41)
\end{aligned}$$

Using the differentiations of equations (23–25) with respect to the rapidities and using equations (38–40), we can recast (41) into the simple formula with the use of the pseudo-energy of the real spin rapidity at thermal equilibrium,

$$\epsilon_c(\lambda_p,\lambda_h)=\varepsilon_1'(\lambda_p)-\varepsilon_1'(\lambda_h). \qquad (42)$$

Note that in the limit of $T\to 0$, the expression (42) coincides with the excitation energy from the ground state. The elementary excitations concerning other kinds of string solutions can be formulated for the charge excitation as well. But in the limit of $T\to 0$, such excitations vanish and only the excitation for the real spin rapidity remains. Hence, the present formulation for the spin and the charge excitations at finite temperatures is a natural extension of the case of $T=0$.

4 Spectral densities of the elementary excitations

First we consider the relation between the origin of the excitation energy and the repidities k_h in (37) and λ_p in (42). At zero temperature, the real charge and the real spin rapidities occupy fully the region $[-\infty, q_c]$ and $[q_s, \infty]$, respectively. In this case, the spin excitation energy is obtained by fixing k_h at q_c, and the charge excitation energy is obtained by fixing λ_p at q_s. It is noted that the pseudo-energies of the real charge and spin rapidities satisfy the conditions $\kappa(q_c) = 0$ and $\varepsilon_1(q_s) = 0$, in the limit of $T \to 0$. At finite temperatures, however, a clear cut-off of the rapidity does not exist and we can take arbitral values of k_h and λ_p in the expressions (37) and (42), because the particle states and the hole states are distributed randomly. To determine the origin of the excitation energy, we extend the above relations between the pseudo-energy and the cut-off of the rapidity to the case of finite temperatures: we take k_h to satisfy $\kappa(k_h) = 0$ for the spin excitation, and λ_p to satisfy $\varepsilon_1'(\lambda_p) = 0$ for the charge excitation. Therefore, the spin excitation energy and the charge excitation energy take the forms as

$$\epsilon_s(k_p) = \kappa(k_p), \tag{43}$$

$$\epsilon_c(\lambda_h) = -\varepsilon_1'(\lambda_h). \tag{44}$$

In the following, we use the excitation energy given by (43) and (44).

The spin excitation spectrum is defined by counting the hole state in the given range of the excitation energy $[\epsilon, \epsilon + d\epsilon]$, since the spin excitation is obtained by adding one rapidity k_p to an unoccupied state at thermal equilibrium:

$$D_s(\epsilon(k)) = \frac{\rho_{\rm I}^h(k)}{|d\epsilon(k)/dk|}, \tag{45}$$

where $\epsilon(k) = \kappa(k)$ and $\rho_{\rm I}^h(k)$ denotes the impurity part of the distribution function at thermal equilibrium. On the other hand, the charge excitation spectrum is defined by counting the particle state, since the charge excitation is obtained by removing one rapidity λ_h from the particle states:

$$D_c(\epsilon(\lambda)) = \frac{\sigma_{1\rm I}'(\Lambda)}{|d\epsilon(\lambda)/d\lambda|}, \tag{46}$$

where $\epsilon(\lambda) = -\varepsilon_1'(\lambda)$ and $\sigma_{1\rm I}'(\Lambda)$ denotes the impurity part of the distribution function at thermal equilibrium.

To see the temperature dependences of $D_s(\epsilon(k))$ and $D_c(\epsilon(\lambda))$ clearly, we further introduce the whole excitation spectrums by counting whole states in $[\epsilon, \epsilon + d\epsilon]$:

$$D_s^{whole}(\epsilon(k)) = \frac{\rho_{\rm I}(k) + \rho_{\rm I}^h(k)}{|d\epsilon(k)/dk|}, \tag{47}$$

$$D_c^{whole}(\epsilon(\lambda)) = \frac{\sigma_{1\rm I}'(\Lambda) + \sigma_{1\rm I}'^h(\Lambda)}{|d\epsilon(\lambda)/d\lambda|}\,. \tag{48}$$

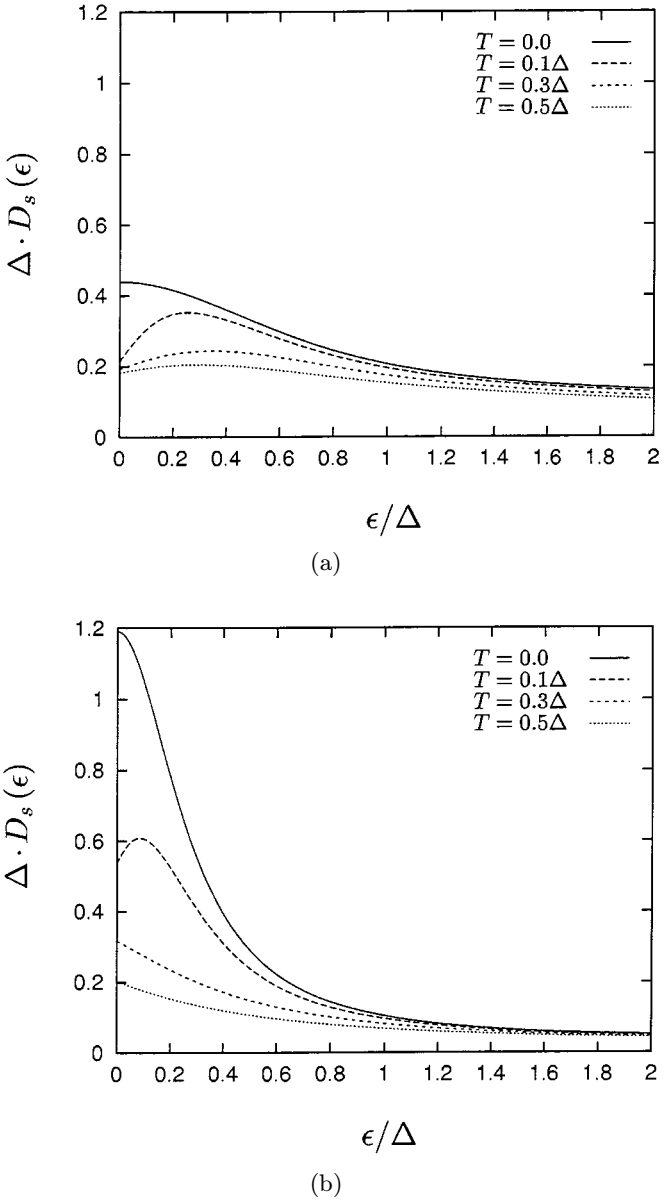

Fig. 1. The numerical results for the spin excitation spectrums are shown in the symmetric case of (a) $U = 1.0\Delta$ and (b) 4.0Δ. $T_K \sim 0.277\Delta$ for $U = 4.0\Delta$.

These excitation spectrums satisfy the following relations:

$$D_s(\epsilon(k)) = \frac{1}{1 + \exp(\epsilon(k)/T)} D_s^{whole}(\epsilon(k)), \tag{49}$$

$$D_c(\epsilon(\lambda)) = \frac{1}{1 + \exp(\epsilon(\lambda)/T)} D_c^{whole}(\epsilon(\lambda)). \tag{50}$$

We solve the equations (16–18) and (23–25) numerically and calculate the elementary excitation spectrums.

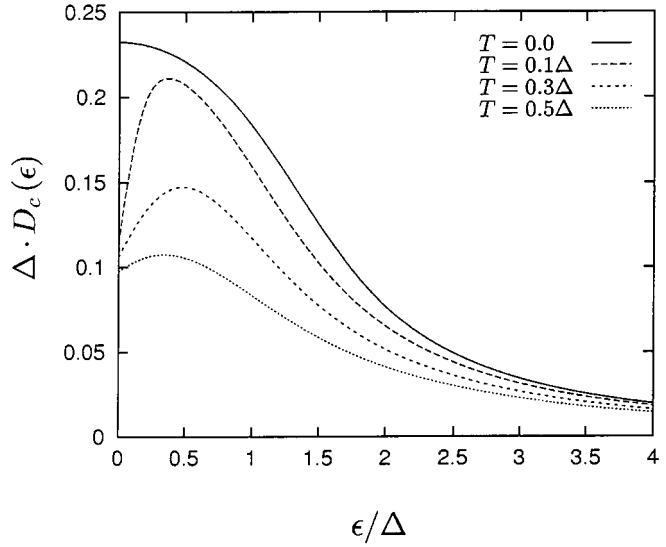

(a)

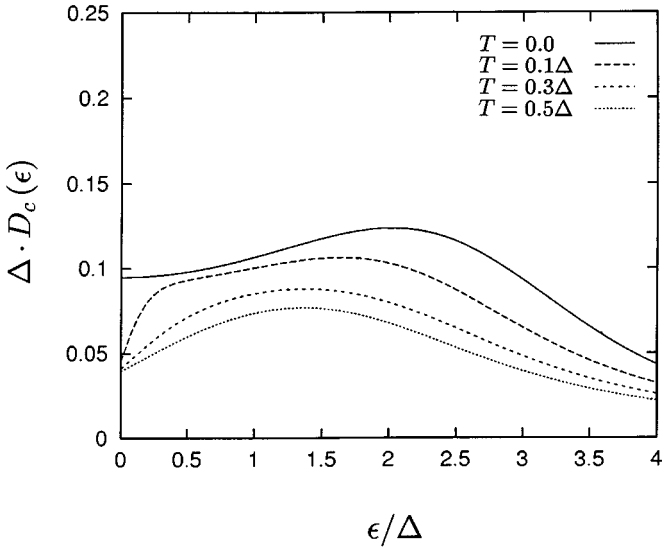

(b)

Fig. 2. The numerical results for the charge excitation spectrums are shown in the symmetric case of (a) $U = 1.0\Delta$ and (b) 4.0Δ. $T_K \sim 0.277\Delta$ for $U = 4.0\Delta$.

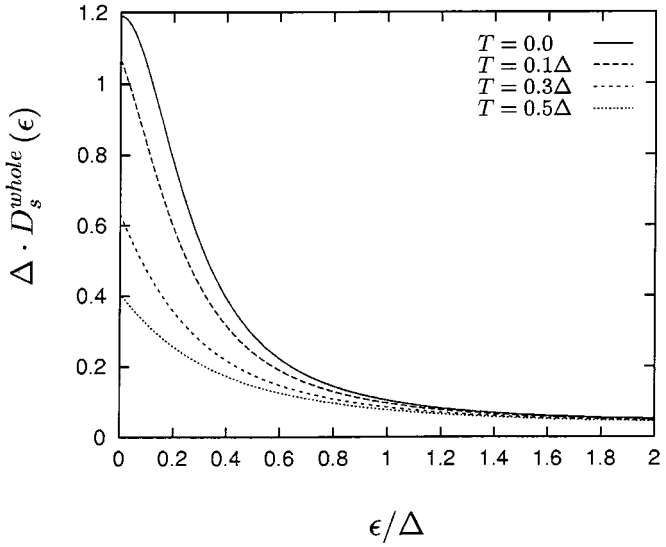

(a)

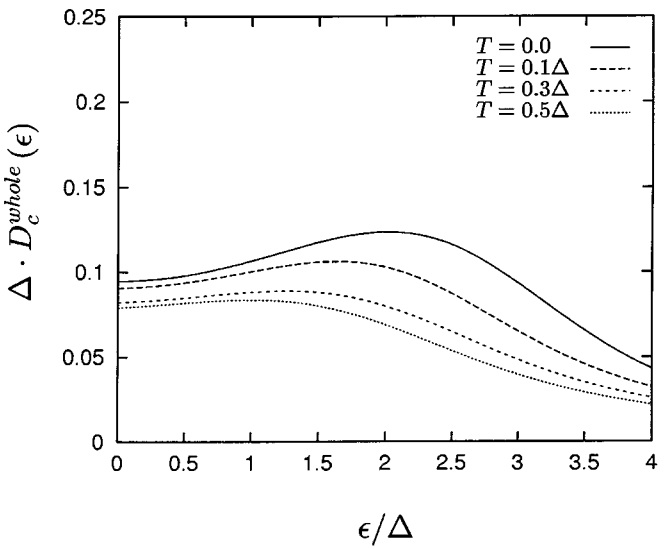

(b)

Fig. 3. The numerical results for the whole excitation spectrums of (a) the spin excitation and (b) the charge excitation are shown in the symmetric case of 4.0Δ. $T_K \sim 0.277\Delta$.

4.1 Symmetric case

The results for the spin excitation spectrums in the symmetric case are shown in Figure 1 for $U = 1.0\Delta$ and $U = 4.0\Delta$. When temperature is decreased below the Kondo temperature, which is given as $T_K = \left(\frac{2\Delta U}{\pi^2}\right)^{1/2} \exp\left[-\frac{\pi}{4}\left(\frac{U}{2\Delta} - \frac{2\Delta}{U}\right)\right] \sim 0.277\Delta$ for $U = 4.0\Delta$, the resonant peak structure grows in the low energy region. This peak structure develops and becomes narrow as the Coulomb interaction increases. The peak structure shown here is related to a characteristic temperature dependence of physical quantities such as the maximum structure of the specific heat around T_K [9].

The charge excitation spectrums are shown in Figure 2 for $U = 1.0\Delta$ and $U = 4.0\Delta$. For the weak Coulomb interaction $U = 1.0\Delta$, the spectrum approaches to the Lorentz-type structure with decreasing temperature. For the strong Coulomb interaction $U = 4.0\Delta$, the hump structure develops around the impurity level $\epsilon_d = -U/2$, reflecting the suppression of the charge fluctuation at low temperatures.

In Figure 3, the numerical results for the whole excitation spectrums $D_s^{whole}(\epsilon(k))$ and $D_c^{whole}(\epsilon(\lambda))$ are shown for $U = 4.0\Delta$. The temperature dependence of $D_s^{whole}(\epsilon(k))$ and $D_c^{whole}(\epsilon(\lambda))$ is not so conspicuous in contrast to that of $D_s(\epsilon(k))$ and $D_c(\epsilon(\lambda))$ in low energy

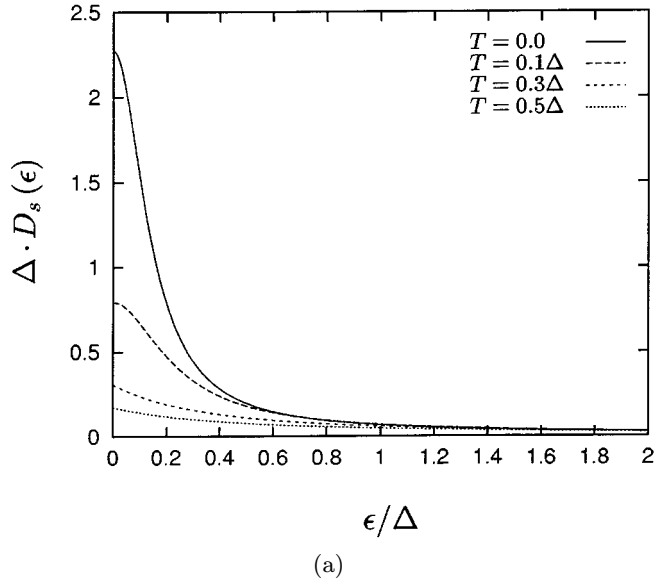

(a)

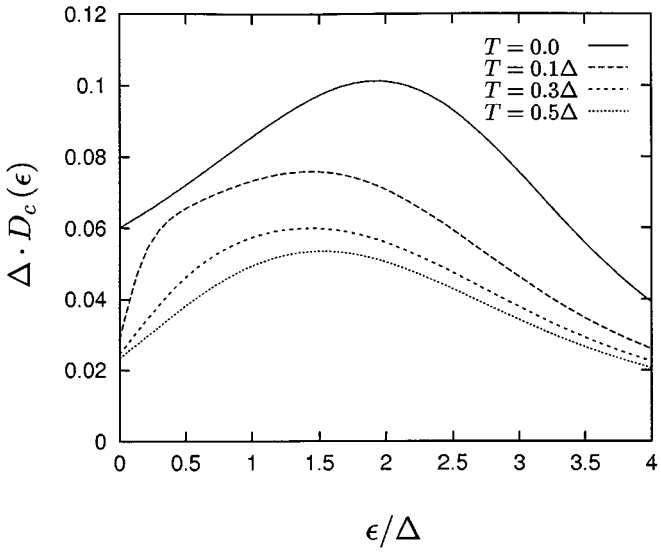

(b)

Fig. 4. The numerical results for (a) the spin excitation spectrums and (b) the charge excitation spectrums are shown for $U = 8.0\Delta$ and $\epsilon_d = -2.0\Delta$. $T_K \sim 0.120\Delta$.

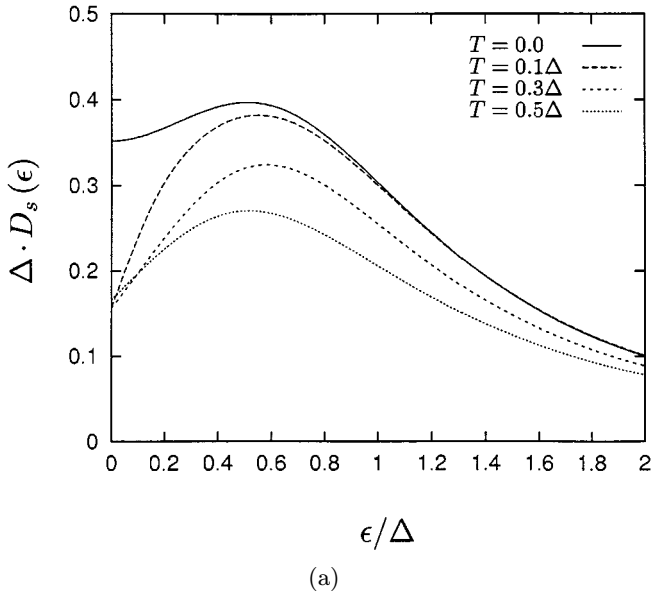

(a)

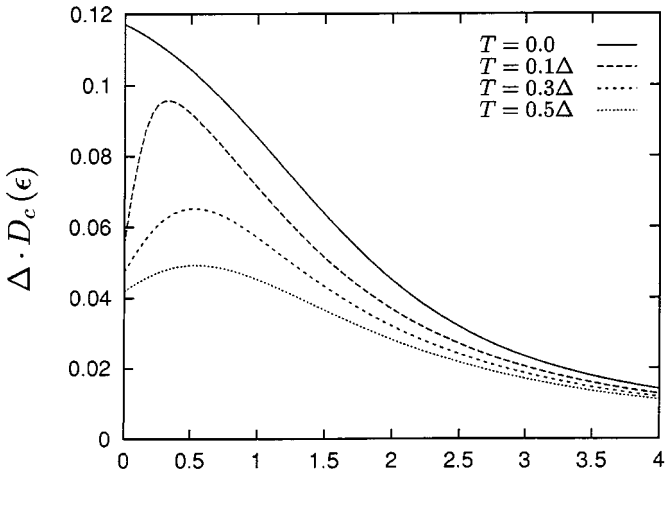

(b)

Fig. 5. The numerical results for (a) the spin excitation spectrums and (b) the charge excitation spectrums are shown for $U = 4.0\Delta$ and $\epsilon_d = 0.0$.

region. From the relations (49, 50), it is considered that the temperature dependence of $D_s(\epsilon(k))$ and $D_c(\epsilon(\lambda))$ in low energy region is caused by the steep gradient of the "Fermi distribution function" close to $\epsilon = 0$.

4.2 Asymmetric case

The numerical results for the spin and the charge excitation spectrums of the asymmetric case with the strong Coulomb interaction ($U \gg \Delta, |\epsilon_d|$) are shown in Figures 4 and 5. When the impurity level lies suitably deep and $|\epsilon_d| > \Delta$ ($U = 8.0\Delta$ and $\epsilon_d = -2.0\Delta$), we can see the resonant peak structure develops in the spin excitation spectrum below T_K, where $T_K = \left(\frac{2\Delta U}{\pi^2}\right)^{1/2} \exp\left[\pi\epsilon_{\rm d}\left(\frac{\rm U+\epsilon_d}{\rm 2\Delta U}\right)\right] \sim 0.120\Delta$ in this case. In the charge excitation spectrum, the hump structure grows around the impurity level with decreasing temperature. When the impurity level lies close to the Fermi energy and $|\epsilon_d| < \Delta$ ($U = 4.0\Delta$ and $\epsilon_d = 0.0$), on the contrary, the resonant peak structure does not grow in the low energy region of the spin excitation spectrum and the charge excitation spectrum approaches the Lorentz-type structure with decreasing temperature. The difference of

the temperature dependence of the excitation spectrums between both cases is caused by the difference of the physical property. In the former case, the charge fluctuation becomes suppressed and the spin fluctuation survives in the low temperature region. Consequently the specific heat, for example, shows a Schottky-type peak around T_K [10]. In this case, the ground state has nearly integer valence. In the latter case, the Kondo effect disappears and the ground state with intermediate valence comes out.

5 Summary

We have studied the elementary excitation spectrums for the Anderson model at finite temperatures by using the Bethe-ansatz solution. Dressed particles are introduced for the formulation of the elementary excitation at finite temperatures. We have discussed the temperature dependence of the spin and the charge excitation spectrums in connection with bulk quantities of low energy region.

It is a great pleasure for us to have been asked to participate in this volume dedicated to Professor J. Zittartz.

References

1. A.M. Tsvelick, P.B. Wiegmann, Adv. Phys. **32**, 453 (1983).
2. A. Okiji, N. Kawakami, in *Theory of Heavy Fermions and Valence Fluctuations*, edited by T. Kasuya, T. Saso, Springer Series in Solid State Science Vol. **62** (Springer-Verlag, Berlin, 1985), pp. 46 and 57.
3. A.C. Hewson: *The Kondo Problem to Heavy Fermion* (Cambridge University Press, Cambridge, 1993).
4. *Dynamical processes and Ordering on Solid Surfaces*, edited by A. Yoshimori, M. Tsukada, Springer Series in Solid State Science, Vol. 59 (Springer-Verlag, Berlin, 1985).
5. K. Yosida, K. Yamada, Prog. Theor. Phys. Suppl. **46**, 244 (1970); K. Yamada, Prog. Theor. Phys. **53**, 970 (1975); K. Yosida, K. Yamada, *ibid.* **53**, 1286 (1975); K. Yamada, *ibid.* **54**, 316 (1975).
6. H.R. Krishna-murthy, J.W. Wilkins, K.G. Wilson, Phys. Rev. B **21**, 1003 (1980) and *ibid.* 1044.
7. P.B. Wiegmann, Phys. Lett. A **80**, 163 (1980).
8. N. Kawakami, A. Okiji, Phys. Lett. A **86**, 483 (1981).
9. A. Okiji, N. Kawakami, Phys. Rev. Lett. **50**, 1157 (1983).
10. N. Kawakami, A. Okiji, Phys. Lett. A **98**, 54 (1983); Phys. Rev. Lett. **51**, 2011 (1983).
11. R.N. Silver, J.E. Gubernatis, D.S. Sivia, M. Jarrell, Phys. Rev. Lett. **65**, 496 (1990); J. Bonča, J.E. Gubernatis, Phys. Rev. B **47**, 13137 (1993).
12. T.A. Costi, A.C. Hewson, Philos. Mag. B **65**, 1165 (1992); T.A. Costi, A.C. Hewson, J. Phys.-Cond. **30**, 361 (1993); T.A. Costi, A.C. Hewson, V. Zlatić, J. Phys.-Cond. **6**, 2519 (1994).
13. O. Sakai, S. Suzuki, Y. Shimizu, Physica B **206, 207**, 141 (1995).
14. C.N. Yang, C.P. Yang, J. Math. Phys. **10**, 1115 (1969).
15. J. des Cloizeaux, J.J. Pearson, Phys. Rev. **128**, 2131 (1962).
16. M. Yamashita, A. Okiji, N. Kawakami, J. Phys. Soc. Jpn **61**, 180 (1992); S. Suga, A. Okiji, N. Kawakami, Phys. Rev. B **50**, 12599 (1994); Y. Morita, S. Suga, A. Okiji, J. Phys.-Cond. **8**, 1753 (1996).
17. N. Kawakami, A. Okiji, Phys. Rev. B **42**, 2383 (1990).
18. S. Fujimoto, N. Kawakami, S.-K. Yang, Phys. Rev. B **50**, 1046 (1994).
19. N. Kawakami, A. Okiji, Solid State Commun. **43**, 467 (1982); V.M. Filyov, A.M. Tsvelick, P.B. Wiegmann, Phys. Lett. A **89**, 157 (1982).
20. A.M. Tsvelick, P.B. Wiegmann, Phys. Lett. A **87**, 368 (1982); N. Kawakami, A. Okiji, J. Phys. Soc. Jpn **52**, 1119 (1983).